GREEN SYNTHESIS OF IRON NANOPARTICLES BY *TERMINALIA CATAPPA* EXTRACTION FOR THE DEGRADATION OF RHODAMINE B IN WASTEWATER

Đến tòa soạn: 21-05-2025

Nguyen Thi Hoai Phuong[1], Truong Ngoc Tuan[2], Dang Minh Quang[1], Nguyen Thi Phuong[3], Nguyen Manh Ha[4], La Duc Duong[3,*]

[1]*Department of Chemistry and Environment, Joint Vietnam-Russia Tropical Science and Technology Research Center*

[2]*Institute of Technology, Vietnam Defence Industry*

[3]*Institute of Materials, Biology and Environment, Academy of Military Science and Technology*

[4]*Faculty of Chemical Technology, Hanoi University of Industry*

**E-mail: duc.duong.la@gmail.com*

TÓM TẮT

TỔNG HỢP XANH HẠT NANO SẮT BẰNG DỊCH CHIẾT LÁ BÀNG (TERMINALIA CATAPPA) ĐỂ PHÂN HỦY RHODAMINE B TRONG NƯỚC THẢI

Trong những năm gần đây, việc sản xuất các hạt nano kim loại thân thiện với môi trường đã phát triển như một hướng thay thế khả thi cho các quy trình hóa học truyền thống. Nghiên cứu này tập trung vào việc tổng hợp xanh các hạt nano sắt (FeNPs) sử dụng các tác nhân khử có nguồn gốc thực vật, với mục tiêu xây dựng một phương pháp hiệu quả và thân thiện môi trường để phân hủy các thuốc nhuộm huỳnh quang thường gặp trong nước thải công nghiệp. Các hạt FeNPs tổng hợp được đặc trưng bằng các phương pháp SEM, XRD và EDX để xác định hình thái, cấu trúc tinh thể và đặc tính chức năng bề mặt. Hiệu suất phân hủy của vật liệu được đánh giá đối với thuốc nhuộm Rhodamine B trong nhiều điều kiện khác nhau, bao gồm pH, liều lượng và nồng độ ban đầu. Kết quả cho thấy các hạt FeNPs tổng hợp xanh thể hiện hoạt tính xúc tác cao và tốc độ phân hủy nhanh, giúp giảm đáng kể nồng độ thuốc nhuộm trong thời gian ngắn. Nghiên cứu động học cho thấy quá trình phân hủy tuân theo mô hình giả bậc hai ($R^2 = 0,94907$) tốt hơn mô hình giả bậc nhất ($R^2 = 0,75665$), gợi ý rằng cơ chế phản ứng chủ yếu là hấp phụ hóa học. Các hạt FeNPs xanh thể hiện tiềm năng cao như một chất xúc tác chi phí thấp, thân thiện môi trường trong xử lý thuốc nhuộm, mở ra hướng ứng dụng khả thi trong xử lý nước thải và kiểm soát ô nhiễm trong các ngành dệt nhuộm. Phương pháp này không chỉ hạn chế sản phẩm phụ độc hại mà còn thúc đẩy nguyên tắc kinh tế tuần hoàn thông qua việc tận dụng nguồn tài nguyên tái tạo trong tổng hợp vật liệu nano.

Từ khóa*:* *tổng hợp xanh, hạt nano sắt, thuốc nhuộm huỳnh quang, phân hủy xúc tác.*

1. INTRODUCTION

The pollution of aquatic ecosystems with synthetic dyes has emerged as a significant environmental concern, especially owing to the widespread application of fluorescent indicator dyes in the textile, biomedical, and analytical sectors. These dyes exhibit great visibility at low concentrations and possess chemical stability, rendering them resistant to standard wastewater treatment methods. Their persistence in aquatic environments could result in significant ecological harm and present toxicological threats to both aquatic creatures and humans [1]. Commonly used fluorescent tracers in Normandy's karstic chalk degraded under chlorination and natural conditions, producing byproducts with low to moderate ecotoxicity [3].

Recent nanotechnology advances made iron nanoparticles (FeNPs) efficient environmental remediation agents, notably for catalytic destruction of organic contaminants [5-7]. FeNPs reduced well, having a large surface area, and being magnetically separable. Conventional chemical synthesis used harmful reducing agents and stabilizers, which contradicted pollution control goals. Green synthesis used plant-based materials rich in bioactive chemicals to decrease and stabilize nanoparticles [8]. Green-synthesized iron nanoparticles using *Vernonia amygdalina* leaf extract were effective, stable, and eco-friendly catalysts for degrading organic dyes with high efficiency and reusability [9]. Iron nanoparticles synthesized from *Artocarpus heterophyllus* peel extract served as effective, eco-friendly Fenton-like catalysts, achieving 87.5% degradation of Fuchsin Basic dye in 20 minutes [10]. *Terminalia catappa*, though underutilized, was a promising plant source whose leaf tannins, flavonoids, and polyphenols effectively reduced metal ions and stabilized nanoparticles [11, 12]. While *Terminalia catappa*-derived Fe NPs were not directly studied for dye degradation, but their extract-derived different nanoparticles were photocatalytic. For example, *Terminalia catappa* leaf extract-synthesized Cu_2O nanoparticles effectively degraded methylene blue dye under visible light, suggesting their potential in wastewater remediation [13]. The green production of iron nanoparticles using *Terminalia catappa* leaf extract was sustainable and promising for medical and environmental applications. Further study on these nanoparticles in dye degradation and wastewater treatment might reveal their practical use.

This study presented the innovative application of *Terminalia catappa* leaf extract for the eco-friendly manufacture of iron nanoparticles and assessed their efficacy in degrading fluorescent indicator colors. The utilization of *Terminalia catappa* for nanoparticle synthesis presented a distinctive amalgamation of elevated phytochemical content, accessibility, and ecological significance. This simultaneous emphasis on a sustainable synthesis process and practical dye degradation application highlighted the originality and ecological importance of our research.

2. EXPERIMENT

2.1. Raw Materials and Chemicals

Fresh, pest-free, and uncontaminated leaves of *Terminalia catappa* were harvested, washed with water, sliced (1 cm), desiccated, and finely pulverized (100 µm).

Iron (III) chloride, Rhodamine B, and ethanol utilized in the research were of analytical grade and procured from Xilong (China). NaOH and HCl utilized were of analytical grade sourced from Merck. Distilled water was utilized for the creation of solutions.

2.2. *Terminalia catappa* leaf extraction

50 grams of *Terminalia catappa* leaves were weighed in a glass beaker, and the dried leaf powder was dissolved in 1 liter of ethanol using ultrasonic waves for 30 minutes. The suspension was heated to 60 °C for 2 hours, subsequently filtered through filter paper and centrifuged to eliminate residue. The extract was maintained at ambient temperature.

2.3. Synthesis of zero-valent iron nanoparticles

6.75 g of $FeCl_3{\cdot}6H_2O$ was dissolved in 25 mL of distilled water and agitated until the solution achieved full homogeneity. Subsequently, 50 mL of *Terminalia catappa* leaf extract was gradually included in the mixture while maintaining continuous agitation for 2 hours to facilitate the reduction of Fe^{3+} to Fe^0 through the influence of polyphenol components present in the extract. The mixture was thereafter allowed to keep overnight at room temperature to finalize the reduction process and produce iron nanoparticles. The product was subsequently recovered via filtration, rinsed multiple times with distilled water to eliminate contaminants and reaction byproducts, and then centrifuged at 6000 rpm for 20 minutes to yield the material precipitate.

2.4. Characterization of Fe^0 nanoparticles

The morphology of the material was examined using scanning electron microscopy (SEM) techniques with magnification capabilities of up to 100,000 times. The crystal structure of the Fe^0 nanoparticles was examined using X-ray diffraction (XRD). The copper X-ray tube (Cu-Kα) operates at 1.54 Å, with a current of 44 mA and a voltage of 40 kV, within the 2θ range of 10° to 80°.

2.5. Rhodamine B removal

The degradation of Rhodamine B (RhB) utilizing Fe NPs was performed under regulated laboratory settings to assess the catalytic efficacy of the material. In a standard experiment, a specified concentration of RhB solution (often between 2.5 and 15 mg/L) was generated in a constant volume, typically 100 mL. A precise quantity of Fe NPs catalyst (ranging from 0.05 to 0.30 g/L) was subsequently introduced to the solution, and the mixture was agitated at a consistent velocity (about 150–200 rpm) at ambient temperature. At specified time intervals of 120 minutes, samples were extracted and promptly filtered or centrifuged to eliminate the solid catalyst. For the experiment to evaluate the effect of initial concentration on Rhodamine B removal efficiency, the time points used for data collection were 15, 30, 45, 60, 75, 90 and 120 min. The residual concentration of RhB in the solution was quantified utilizing a UV-Vis spectrophotometer at the peak absorbance wavelength of 553 nm.

The efficiency of RhB removal on Fe NPs was calculated by the following equation:

$$H\ \% = \frac{(C_0 - C_t)}{C_0} \times 100\% \quad (1)$$

where C_0 and C_t (mg/L) were the initial and residual RhB concentrations, respectively.

The first-order kinetic model was employed to simulate experimental data to ascertain the surface photodegradation rate constant:

$$\frac{C_t}{C_0} = e^{-k_1 t} \quad (2)$$

The second-order kinetic model was utilized to simulate the elimination kinetics of RhB by Fe NPs in solution:

$$\frac{C_t}{C_0} = \frac{1}{1 + k_2.C_0.t} \quad (3)$$

where C_0, C_t (ppm) were concentration of RhB at intial and t moment, respectively; k_1 (min^{-1}) was the pseudo-first-order rate constant; k_2 ($L.(mg.min)^{-1}$) was the pseudo-second-order rate constant.

3. RESULTS AND DISCUSSION

3.1. Characterization of Fe NPs

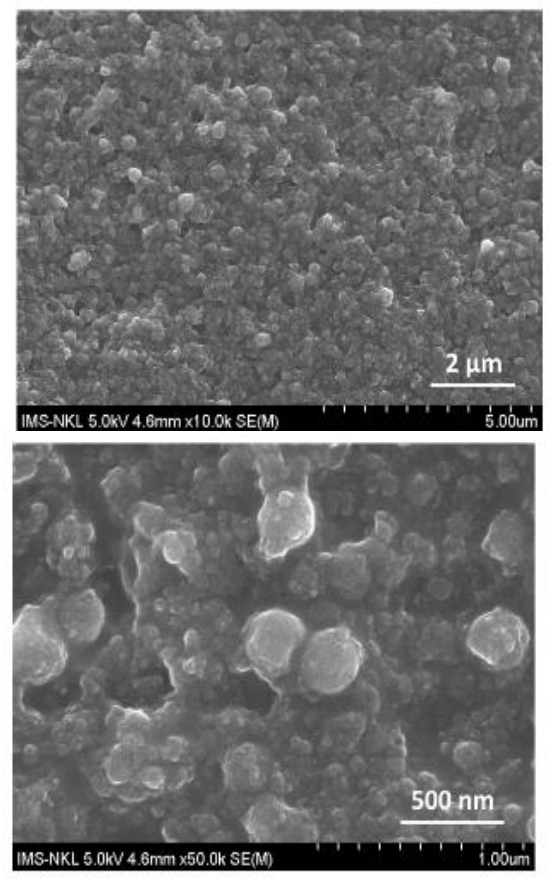

Figure 1. *SEM image of Fe NPs synthesized with Terminalia catappa leaf extract.*

The SEM image of Fe nanoparticles (Fe NPs) synthesized using *Terminalia catappa* (TC) leaf extract revealed predominantly spherical to quasi-spherical particles with sizes estimated at 50÷200 nm (Figure 1). The nanoparticles exhibited relatively smooth surfaces and moderately uniform size distribution, suggesting effective bioreduction and stabilization by phytochemicals present in the TC extract. Agglomeration was visible, likely due to magnetic interactions or partial surface capping by organic compounds. Overall, the morphology indicated successful green synthesis, with natural biomolecules facilitating the formation and stabilization of Fe NPs under mild, eco-friendly conditions.

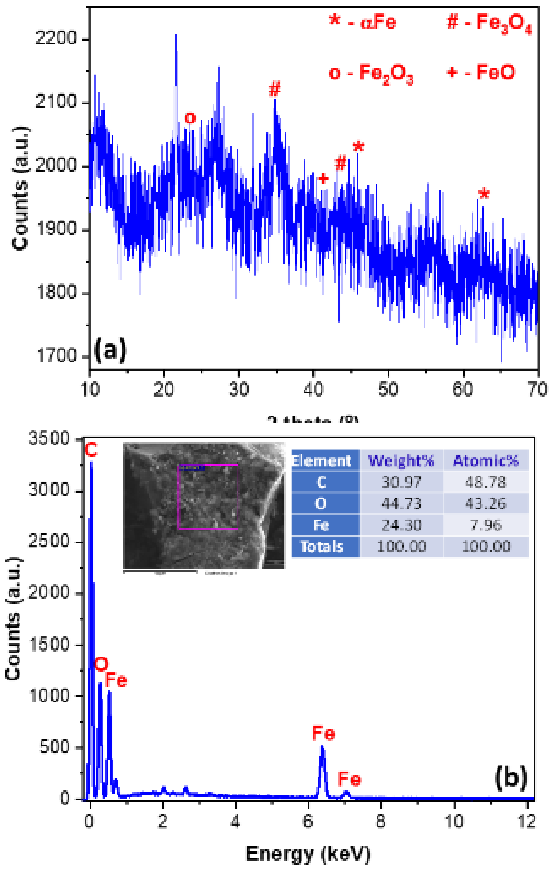

Element	Weight%	Atomic%
C	30.97	48.78
O	44.73	43.26
Fe	24.30	7.96
Totals	100.00	100.00

Figure 2. *XRD pattern (a) and EDX spectroscopy (b) of Fe NPs synthesized with Terminalia catappa leaf extract.*

The XRD pattern of Fe NPs shown in Figure 2a exhibited broad and low-intensity peaks, indicating the nanoscale nature and partial amorphous character of the sample. Distinct diffraction peaks corresponded to multiple iron phases, including metallic α-Fe (PDF 00-006-0696), Fe_3O_4 (magnetite, PDF 00-065-0731), Fe_2O_3 (hematite, PDF 00-013-0534), and FeO (wüstite, PDF 00-046-1312). The presence of these multiple phases suggested that the green synthesis using *Terminalia catappa* extract led to partial oxidation of iron, resulting in a mixture of iron and iron oxide phases. This phase diversity was typical for biologically synthesized Fe NPs, where phytochemicals acted as both reducing and stabilizing agents under ambient conditions. The EDX spectrum of Fe NPs in Figure 2b confirmed the elemental composition of the sample, primarily consisting of carbon (C), oxygen (O), and iron (Fe). The prominent peaks for Fe indicated the successful incorporation of iron in the nanoparticle structure, while the substantial presence of oxygen suggested partial oxidation, consistent with the formation of iron oxides (as also observed in the XRD results). The high carbon content, with a weight percentage of 30.97%, likely originated from organic compounds in the *Terminalia catappa* leaf extract used during green synthesis, which acted as capping and stabilizing agents. The atomic percentages further showed that Fe was present at 7.96%, with O and C dominating the surface, suggesting that the nanoparticles were coated with a bio-organic layer. Overall, the EDX analysis supported the formation of biofunctionalized iron-based nanoparticles.

3.2. Rhodamine B removal with Fe NPs

Figure 3 illustrated that Rhodamine B (RhB) degradation efficiency (H%) increased over time for all initial concentrations, with a noticeable slowdown after around 60 minutes, suggesting the approach to equilibrium. At low concentrations, there were fewer RhB molecules available to occupy the catalytic sites, leading to a faster decomposition and higher initial yields. In contrast, at high concentrations, an increased number of RhB molecules competed for adsorption, which could exceed the immediate reaction capacity of the material, resulting in lower initial yields. Lower initial concentrations (2.5 and 5.0 mg/L) achieved the highest efficiencies, reaching about 98% and 96% at 120 minutes, respectively, due to the greater availability of active sites relative to dye molecules. As the initial concentration increased, the degradation efficiency decreased, with 15.0 mg/L showing the lowest final H% (~84%), likely due to the saturation of active sites and possible mass transfer limitations. This indicated that the degradation system was more effective at lower dye concentrations, while higher concentrations hindered performance due to limited reactive capacity.

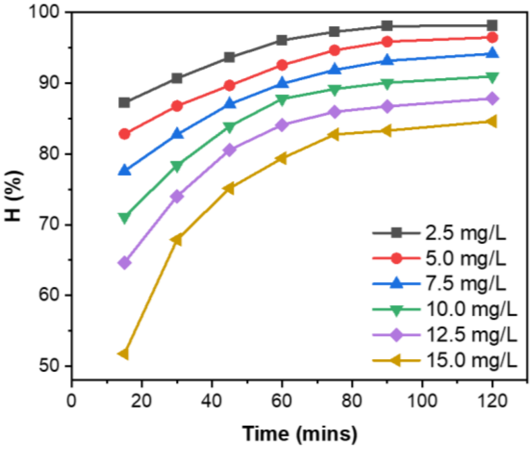

Figure 3. *RhB degradation efficiency over time with different initial concentrations.*

Figure 4a showed the effect of different dosages of Fe NPs on RhB degradation efficiency (H%) after 120 minutes. As the Fe NPs dosage increased from 0.25 to 1.0 g/L, H% rose significantly from around 62% to approximately 91%, indicating enhanced catalytic activity due to the increased number of reactive sites available for degradation. Beyond 1.0 g/L, the efficiency plateaus, with only slight increased, observed up to 1.5 g/L, suggesting that excessive Fe NPs might lead to particle agglomeration or light scattering effects that limited further improvement. Therefore, 1.0 g/L appeared to be the optimal dosage, balancing high degradation efficiency and material economy.

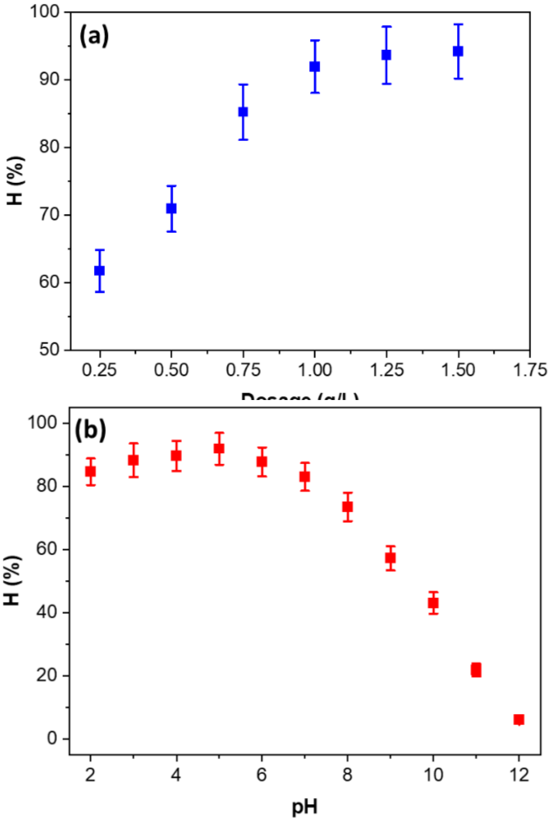

Figure 4. *RhB degradation efficiency with different dosages of Fe NPs for 120 mins.*

Figure 4b demonstrated the effect of pH on RhB degradation efficiency (H%) using Fe NPs over 120 minutes. The degradation efficiency remained high (~85–92%) in the acidic to neutral range (pH 2–6), with a peak observed around pH 5, indicating optimal conditions for Fe NPs activity and ROS (reactive oxygen species) generation. As the pH increased beyond 6, H% began to decline sharply, dropping to around 75% at pH 8 and falling drastically to below 10% at pH 12. The reduced efficiency in alkaline conditions might result from the precipitation of iron hydroxides, lower availability of Fe^{2+}, and decreased generation of •OH radicals. This suggested that acidic conditions favor RhB degradation with Fe NPs, while alkaline environments significantly hindered the process.

The degradation kinetics of RhB by Fe NPs were evaluated using pseudo-first-order and pseudo-second-order models. The pseudo-first-order model (above) yielded a rate constant (k_1 = 0.03984 min^{-1}) with a moderate correlation coefficient (R^2 = 0.75665), indicating a less accurate fit to the experimental data. In contrast, the pseudo-second-order model (under) provided a much better fit, with a rate constant (k_2 = 6.73445 x 10^{-4} $L.g^{-1}.min^{-1}$) and a high correlation coefficient (R^2 = 0.94907). This suggested that the RhB degradation process on Fe NPs was better described by pseudo-second-order kinetics, implying that chemisorption or surface interactions played a dominant role in the reaction mechanism.

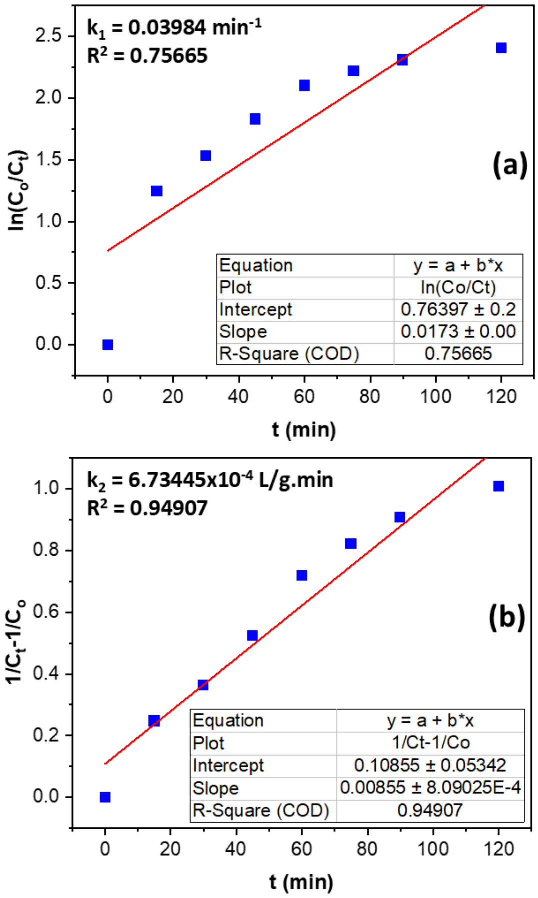

Figure 5. *The first-pseudo order (left) and second-pseudo order (right) models of RhB degradation on Fe NPs.*

The decomposition of RhB (Rhodamine B) using synthetic materials primarily relied on oxidation-reduction processes that generated free radicals. Under exposure to light, electrons from the material were stimulated, leading to the formation of •OH and O_2^{-} • radicals, which are powerful oxidizing agents. These radicals could degrade the aromatic ring structure and chromophore group of RhB molecules, ultimately resulting in complete disintegration. Additionally, the surface of the material, rich in functional groups and active sites, enhanced its catalytic properties. This feature improved the adsorption and interaction between RhB and the oxidizing radicals, facilitating the degradation process.

4. CONCLUSION

In this study, iron nanoparticles (Fe NPs) were successfully synthesized via a green approach and evaluated for their efficiency in degrading fluorescent indicator dyes, using Rhodamine B (RhB) as a model pollutant. The degradation performance was strongly influenced by operational parameters including initial dye concentration, Fe NP dosage, and solution pH. Results demonstrated that lower initial dye concentrations (2.5–5.0 mg/L) yielded the highest degradation efficiencies, while excessive concentrations reduced the removal rate due to active site saturation. An optimal Fe NP dosage of 1.0 g/L was identified, beyond which no significant improvement was observed, likely due to particle agglomeration. Furthermore, the degradation was most efficient under acidic to neutral pH conditions, with a marked decline in alkaline media. These findings highlighted the potential of green-synthesized Fe NPs as an effective and eco-friendly catalyst for the treatment of dye-contaminated wastewater under optimized conditions.

ACKNOWLEDGEMENT

This research was financed by the National Foundation for Science and Technology Development under grant code NCUD.01-2024.15 and conducted at the Joint Vietnam-Russia Tropical Science and Technology Research Center.

REFERENCES

[1] Field, M. S. J. E.; Geoscience, E., (2005). Assessing aquatic ecotoxicological risks associated with fluorescent dyes used for water-tracing studies. **11(4)**, 295-308.

[2] Kieft, T. L.; Byrd, E.; Veni, G. J. G., (2022). Toxicological Study of Fluorescent Hydrologic Tracer Dye Effects on Cave Bacteria. **60(3)**, 404-409.

[3] Gombert, P.; Biaudet, H.; de Seze, R.; Pandard, P.; Carré, J. J. I. J. o. S., **(**2017). Toxicity of fluorescent tracers and their degradation byproducts. **46(1)**, 5.

[4] Sharma, J.; Sharma, S.; Bhatt, U.; Soni, V. J. J. o. H. M. L., **(**2022**).** Toxic effects of Rhodamine B on antioxidant system and photosynthesis of Hydrilla verticillata. **3**, 100069.

[5] Zhou, H.; Wu, S.; Zhou, Y.; Yang, Y.; Zhang, J.; Luo, L.; Duan, X.; Wang, S.; Wang, L.; Tsang, D. C. J. E. i., (2019**).** Insights into the oxidation of organic contaminants by iron nanoparticles encapsulated within boron and nitrogen co-doped carbon nanoshell: Catalyzed Fenton-like reaction at natural pH. **128**, 77-88.

[6] Halligudra, G.; Sabbanahalli, C.; Singh, S.; Choudhary, P.; Tigari, G.; Lo, S.-L. J. J. o. P.; Solids, C. o., (2025**)**. Catalytic behaviour of iron-based nanomaterials for the remediation of hazardous chemicals from wastewater: A Review, 112735.

[7] Chaudhari, D. S.; Upadhyay, R. P.; Shinde, G. Y.; Gawande, M. B.; Filip, J.; Varma, R. S.; Zboril, R. J. G. C., (2024). A review on sustainable iron oxide

nanoparticles: synthesis and application in organic catalysis and environmental remediation.

[8] Kumar, V.; Kaushik, N. K.; Tiwari, S. K.; Singh, D.; Singh, B. J. I. J. o. B. M., **(**2023). Green synthesis of iron nanoparticles: Sources and multifarious biotechnological applications. **253**, 127017.

[9] Jara, Y. S.; Mekiso, T. T.; Washe, A. P. J. S. R., (2024). Highly efficient catalytic degradation of organic dyes using iron nanoparticles synthesized with Vernonia Amygdalina leaf extract. **14(1)**, 6997.

[10] Jain, R.; Mendiratta, S.; Kumar, L.; Srivastava, A. J. C. R. i. G.; Chemistry, S., (2021). Green synthesis of iron nanoparticles using Artocarpus heterophyllus peel extract and their application as a heterogeneous Fenton-like catalyst for the degradation of Fuchsin Basic dye. **4**, 100086.

[11] Mwangi, W. C.; Waudo, W.; Shigwenya, M. E.; Gichuki, J. J. B. C. M., (2024). Therapies, Phytochemical characterization, antimicrobial and antioxidant activities of Terminalia catappa methanol and aqueous extracts. **24(1),** 137.

[12] Sirat, N. M.; Senjaya, A. A. J. J. o. H.; Sciences, M., (2021). Chemical Compound of Terminalia Catappa L. as Hemostatic Agents in Post Tooth Extraction. **4(4)**.

[13] Nguyen, T. H. P.; Nguyen, T. P.; Nguyen, T. A. T.; Nguyen, T. D.; Chang, S. W.; Nguyen, D. D.; La, D. D. J. D. A. S., (2024). Terminalia catappa leaf extract as a bio-reducing agent to synthesize Cu_2O nanoparticles for methylene blue photodegradation. **6(6)**, 309.